

Automation of the EMBL Hamburg protein crystallography beamline BW7B

Ehmke Pohl,^{a*‡} Uwe Ristau,^{a§} Thomas Gehrman,^{a§} Doris Jahn,^a Bernd Robrahn,^a Dirk Malthan,^b Hannes Dobler^b and Christoph Hermes^{a*}

^aEuropean Molecular Biology Laboratory Hamburg Outstation, Notkestrasse 85, D-22603 Hamburg, Germany, and ^bFraunhofer Institute for Manufacturing Engineering and Automation, Nobelstrasse 12, D-70569 Stuttgart, Germany.
E-mail: ehmke.pohl@psi.ch, hermes@embl-hamburg.de

The EMBL Hamburg Outstation currently operates five synchrotron beamlines for protein crystallography. The strongest of these beamlines is the fixed-energy beamline BW7B which receives about half of the radiation (1.5 mrad) from a 56 pole wiggler located at the DORIS III storage ring at the German synchrotron facility DESY. Over the last years this beamline has been upgraded and equipped with a fully automated crystallographic end-station and a robotic sample changer. The current set-up allows for remote operation, controlled from the user's area, of sample mounting, centering and data collection of pre-frozen crystals mounted in Hampton-type cryovials on magnetic caps. New software and intuitive graphical user interfaces have been developed that control the complete beamline set-up. Furthermore, algorithms for automatic sample centering based on UV fluorescence are being developed and combined with strategy programs in order to further automate the collection of entire diffraction data sets.

Keywords: beamline automation; protein crystallography; sample changer; crystal recognition; UV fluorescence.

1. Introduction

Over the last years the automation of synchrotron beamlines for protein crystallography has become an important area of development for a number of reasons. First of all, the demand for synchrotron beam time is still increasing owing to the advances in all steps prior to the diffraction experiment (cloning, protein expression, purification and crystallization), leading to a growing number of projects [reviewed for example by Hendrickson (2000) and Helliwell (2002)]. Also, the various structural genomics endeavors add to this rising demand (Kim, 1998; Stevens *et al.*, 2001; Heinemann *et al.*, 2001; Burley & Bonanno, 2002; Zhang & Kim, 2003; Terwilliger *et al.*, 2003). In addition, more and more projects require the screening of a large number of crystals, for example in the case of membrane proteins or large multi-protein complexes where often only a few out of many crystals diffract reasonably well. Furthermore, in many structure-based drug design projects a large number of protein–ligand complex structures need to be determined. Thus the first goal of the automation projects on all levels is to increase the efficient use of limited synchrotron beam time (Abola *et al.*, 2000; Sweet *et al.*, 2001). Secondly, as the field of protein crystallography is growing, the number of less-experienced users at the synchrotrons is steadily increasing (Mitchell *et al.*, 1999). Thus the success rate of sample mounting and dismounting, and hence the results of the diffraction

experiment can be significantly improved by automation. These efforts are accompanied by the development of appropriate software tools such as intuitive graphical user interfaces and underlying expert systems in order to aid the decision-making process before and throughout a data collection (McPhillips *et al.*, 2002).

During the past few years a number of automation projects have been initiated, mainly at the various synchrotron sites. The central element of all these developments is the crystal or sample changer. In the past, two different designs have been implemented. The sample changers at the Stanford Synchrotron Radiation Laboratory (SSRL) (Cohen *et al.*, 2002), the Advanced Photon Source (APS) and the French beamline for Investigation of Proteins (FIP) at the European Synchrotron Radiation Source (ESRF) (Roth *et al.*, 2002; Ohana *et al.*, 2004) are based on standard industrial robots offering a high degree of flexibility at moderate costs. Here, the robot can select samples from different positions in a storage dewar. In contrast, the systems developed by Abbott Laboratories (Muchmore *et al.*, 2000), at the European Molecular Biology Laboratory, Grenoble, and the ESRF (EMBL/ESRF) (Cipriani, 2003), at DORIS (Karain *et al.*, 2002), the Advanced Light Source (ALS) (Earnest *et al.*, 2002; Rupp *et al.*, 2002) and at SPring-8 (Yamamoto, 2002; Ida *et al.*, 2002) are based on fixed custom-made transport systems where the cryo-frozen samples are moved in the dewar or the entire dewar is moved to the loading/unloading position. In the meantime, commercial sample changers produced by three different companies have become available: the ACTOR by Rigaku/MSK, developed in collaboration with Abbott Laboratories (<http://www.msk.com>), and BruNo by BrukerNonius (<http://www.bruker-axs.com>) are based on industrial six-axis robots whereas the cryogenic sample changer by MarResearch consists of a very compact transport mechanism specially designed for the Mar desktop beamline Dtb (<http://www.marresearch.com>).

In this paper we describe recent upgrades and new designs of the EMBL Hamburg wiggler beamline BW7B (van Silfhout & Hermes, 1994). The automated crystallographic end-station consists of a novel fully motorized ϕ goniostat, an industrial six-axis robot equipped with pneumatic cryotongs and a fixed storage dewar for up to 54 crystals mounted in cryoloops and stored in Hampton magnetic caps with plastic vials. Software tools for (semi-) automated sample centering and hardware solutions for sample tracking will be presented and discussed in the context of standardization among the European synchrotron sources.

2. Experimental set-up

There were a number of specific boundary conditions for the design of the automated end-station and the sample changer at beamline BW7B. (i) The design of the prototype had to be versatile and flexible so that the same system could be easily adopted with minimum effort for any of the other four beamlines for protein crystallography, the wiggler MAD beamline BW7A (Pohl *et al.*, 2001) and the three bending-magnet beamlines X11, X12 and X13 (Hermes *et al.*, 2004). (ii) We expected that a significant number of users would still prefer manual mounting, particularly in challenging projects. Therefore sufficient space had to be kept for the required hardware, for example a small table for the crystallization trays, a set of tools for crystal manipulation and the microscope. This requirement was of particular importance during the set-up and testing phase where the beamline had to be kept open to the general user community. (iii) Owing to the occasionally relatively large shifts in beam position it was essential that the entire system was located on the same experimental table. Using this arrangement the sample changer does not move with

* Current address: Swiss Light Source at Paul Scherrer Institute, CH-5232 Villigen, Switzerland.

‡ These authors contributed equally to this work.

respect to the crystal position during beamline alignment procedures. These specific requirements were met with the modular set-up shown in Fig. 1. The system features a new crystallographic end-station, the Adept six-axis robot (<http://www.adept.com>), the storage dewar for pre-frozen crystals and the Mar imaging-plate detector mounted on a Newport optical table.

2.1. Crystallographic end-station

Compared with the previous end-station the new design features two main improvements (Fig. 2). First, all movements are now motorized and remotely controlled, including the two x,y slit systems comprising the collimator, φ rotation, x,y,z movements of the sample, and beam stop. Secondly, the traditional standard goniometer was replaced by a crystal cap holder [(2), the numbers in brackets refer to the labels in Figs. 2(a) and 2(b)], which is magnetically coupled to the φ axis (Fig. 2a). This compact design allows for a short crystal-detector distance (minimum 85 mm for the current detector) for ultrahigh-resolution data collection without vertical detector offset. Furthermore, the crystal centering option can be performed at any φ rotation angle. A high-precision linear drive (10) with a small electromagnet attached to it (7) is mounted orthogonal to both the φ axis and the viewing axis of the microscope. The set-up allows the crystal cap holder to be pushed and pulled in minimal steps and a reproducibility of approximately 1 μm under video control at any given φ rotation angle. This operation can be repeated after a 90° φ rotation in order to position the sample in the center of rotation. To ensure a smooth approach of the linear drive, a pneumatically activated absolute Heidenhain encoder (<http://www.heidenhain.com>) measures the distance of the tip to the crystal cap holder (8). A second linear Sony encoder (9) located next to the motor is used to control the subsequent movement of the linear drive. As the crystal may have been moved significantly in the centering step (for example because of bent loops), the cap with the sample has to be moved back to the fixed mounting/dismounting position before crystal retrieval. This is elegantly accomplished by a pre-centering device consisting of a tapered metal tube (3) that is moved coaxially to the φ axis over the crystal cap holder (2), thus pushing the entire support back to its original position.

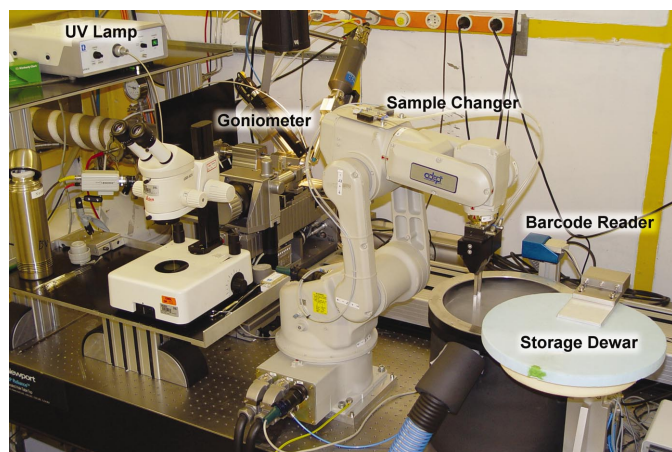


Figure 1
General overview of the automated wiggler beamline BW7B. The crystallographic end-station is located on the left-hand side, the Mar imaging-plate detector is parked in its safe position. The Adept industrial six-axis robot for sample mounting/dismounting and the storage dewar are located in the center of the picture.

The Hampton-type magnet on the tip of the crystal cap holder can easily be exchanged in order to accommodate a small arc for sample exchange or a different magnet (for example the design by Oxford-Cryosystems) in order to offer different options for manual mounting. Besides, a support for the UV light source [see Fig. 1 and (5) in Fig. 2(a)] is added next to the video camera. The fluorescence signal from biological macromolecules can be used for sample detection as described below (Rosenbaum, 2000).

2.2. Robotic sample changer

The sample changer is based on the industrial AdeptSix300 six-axis robot (also designated *Vincent* for ‘versatile industrial crystal elevator and transporter’) with a horizontal and vertical reach of 677 mm and 1019 mm, respectively. With a maximum load of 3 kg and maximum joint speeds between 170 and 300°s^{-1} , the repeatability is 20 μm . Sample mounting/dismounting at a working speed of 50% of the maximum speed requires approximately 3 s. Thus, the sample

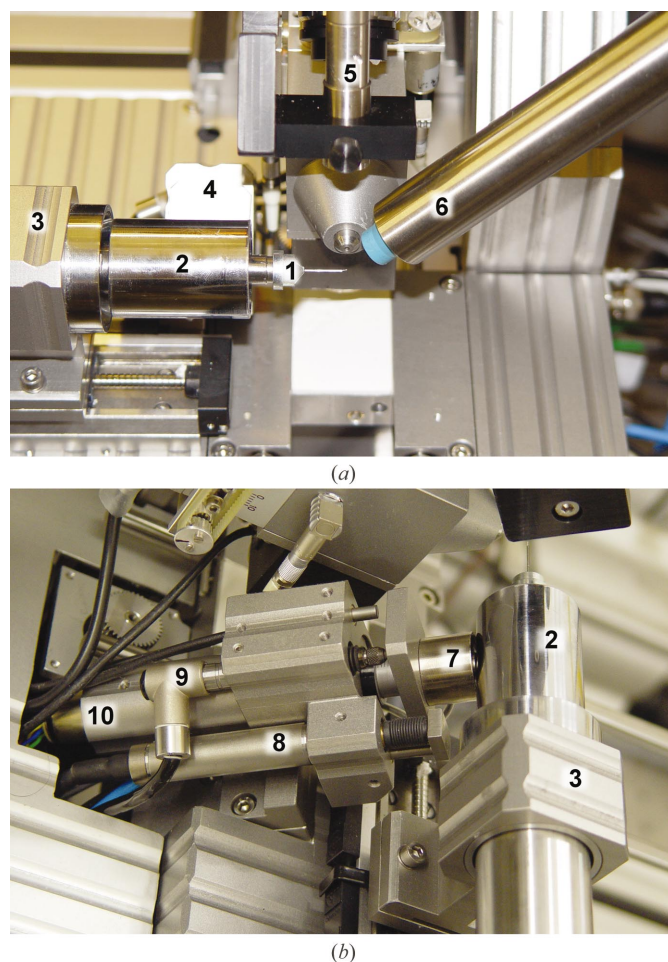


Figure 2
(a) Close-up of the sample environment of the EMBL Hamburg crystallographic end-station. The magnetic crystal cap (1) is shown in the center mounted on the magnetic holder (2) on the φ axis with the centering tube (3). The centering mechanics (4) are positioned perpendicular to the φ axis. The video camera and the UV light fiber optic are mounted at an angle of 45° with respect to the beam direction (5). The cryosystem (6) is located on the right-hand side. During mounting/dismounting the beam stop is moved to its maximum distance to avoid any collision. (b) View along the φ axis showing the centering device consisting of the electromagnet (7), the absolute heidenhain (8) and Sony (9) encoders and the translational motor (10).

centering becomes the time-limiting step when several samples are mounted and dismounted. The robot arm is equipped with pneumatic grippers that are based on cryotongs manufactured by Hampton but optimized for the spatial restraints in the crystal environment on the φ goniostat. All robot movements and sequences of movements are programmed in the robot-programming language V+ which is interfaced to the overall control software coded in C/C++ (see below).

2.3. Sample dewar

At the time of our design studies almost all users arrived with crystal vials mounted on aluminium canes. Besides, several completely different systems for crystal transport had already been introduced. Examples are the ALS puck system where the 16 magnetic caps are mounted without plastic vials and with the metal pins pointing upwards, the ACTOR cassettes with 12 samples arranged in a honeycomb, the EMBL/ESRF baskets with 11 samples on magnetic caps with plastic vials (Cipriani, 2003) and the SSRL system where 96 crystals are stored in a cylindrical cassette (Cohen *et al.*, 2002). We thus decided to start with the compact dewar design depicted in Fig. 3 where the crystal vials are mounted on vertical racks. The custom-made racks can be removed from the dewar and are manually loaded with crystals in the preparation room from any pucks or canes. Further development is currently underway to automate this step when a common puck standard is established (Tucker, 2004).

The storage dewar with the rack holder and the automatic filling system were manufactured using our design by Cryoanlagenbau (<http://www.cryo-system.de>). With the first system that was delivered we experienced severe icing problems, particularly around the top. Therefore, an additional insulation layer, made of Armaflex M19, and a heated rim that keeps the temperature at 313 K were implemented. Furthermore, the top-opening mechanism was improved from a simple vertical movement to a lift-and-turn operation (Fig. 3). Owing to these changes, the system now operates reliably for weeks without ice build-up around the dewar top. Nitrogen consumption greatly depends on the number of mounting/dismounting cycles but averages around 2 l h^{-1} . The crystal-holding dewar is automatically filled from a 60 l liquid-nitrogen storage dewar.



Figure 3
Close-up of the storage dewar in its open position showing the horizontally stored magnetic crystal caps with plastic vials on vertical racks. Each rack can be removed manually and loaded in the user room.

2.4. Graphical user interfaces

Intuitive graphical user interfaces are a vital part of all ongoing automation projects as even the best technology may not be accepted if the usage appears cumbersome. We therefore decided to develop a new software system that controls all steps of the X-ray diffraction experiment from beamline optimization to automated crystal testing and data collection. The new BW7B_control software written in C/C++ combines three modules. The first module communicates to the mar345 control software running on a DEC station *via* a TCP/IP connection. The actual data collection as well as the display of the recorded diffraction pattern is performed by the mar345 image-plate control software. The second module provides a link to the Robot-Control software and the third module links the BW7B_control to the crystal detection program that is still under development as described below. These modules run on the same PC under Windows2000. In addition, the BW7B_control program operates all beamline axes *via* serial links to intelligent motor controllers.

The main menu of the beamline control software is shown in Fig. 4. The different submenus are arranged as buttons in the first line. *BeamLine* is limited to the internal staff. This submenu includes diagnostics features and table optimization. The *Goniometer* submenu allows the remote control of all motors related to data collection, such as slit settings, detector and beam stop position. The *VincentControl* option allows the mounting and dismounting of individual samples and the *CrystalCentering* option permits the (semi-) automatic centering of a given crystal (mounted either manually or robotically). The *DataCollection* submenu controls all data-collection parameters that are used to start the data collection with the mar345 imaging-plate software. Once the automatic centering (current status and future directions are described in some more detail below) is sufficiently stable the four steps, mounting, centering, data collection (either taking a number of test images or collecting an entire data set by a given number of samples) and crystal retrieval, will be summarized in the *DataCollection* window. Since the software development is still ongoing, further details will be published elsewhere.

3. Performance of the system

3.1. Sample mounting/dismounting

After the storage dewar is manually loaded with two racks of crystals mounted on magnetic Hampton caps with plastic vials, all of

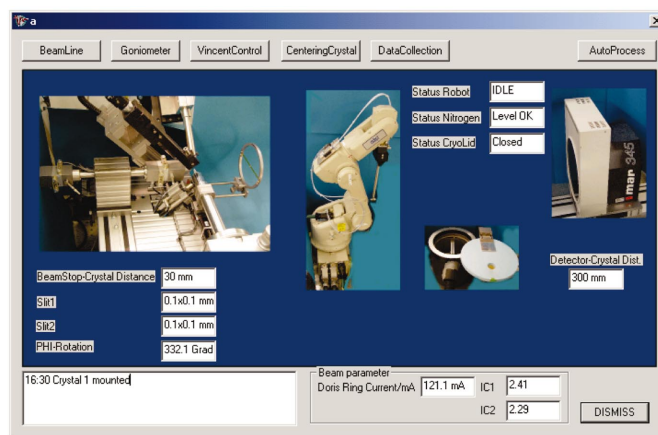


Figure 4
Main graphical user interface showing the main control routines from left to right, *BeamLine*, *Goniometer*, *VincentControl*, *CrystalCentering* and *DataCollection*.

the following operations are remotely controlled. Crystal mounting requires the following steps: (i) The centering tube [labeled (3) in Fig. 2] is moved forward to position the crystal cap holder with the magnet at the fixed mounting/dismounting location. The imaging-plate detector and the beam stop are driven to a safe position in order to avoid any possible collision with the robotic arm. Depending on the actual detector position this step takes up to 20 s (100–800 mm). (ii) The top of the dewar opens and the robot arm moves to the desired crystal cap position. Then, the gripper is precooled under liquid nitrogen for 5 s and after that takes the vial off the magnetic cap. The vial is parked on the empty (0, 0) rack position. (iii) The gripper subsequently grabs the magnetic cap, (iv) drives by the barcode reader (see §3.3) and (v) mounts the crystal on the tip of the φ goniostat. (vi) Finally, the gripper is moved to its parking position. At this point the user may start the semi-automatic centering and consecutively begins the recording of a diffraction pattern. During data collection the gripper can be parked in the dewar to keep it at liquid-nitrogen temperature if necessary. Dismounting is performed in the opposite order without the barcode-reading step. So far, there is no drying step included as the gripper is parked under liquid nitrogen for short waiting times, *e.g.* during crystal testing, and it can dry outside during longer data collection.

3.2. Sample centering and UV fluorescence

At this time the sample centering step is performed semi-automatically. The view of the crystal in the loop is displayed on a second computer screen in the control area and the user selects the center of the sample by a simple mouse click. This position is then moved automatically to the center of rotation. Centering can be performed at any given φ value wherever the crystal is well visible and then repeated at $\varphi + 90^\circ$ and $\varphi + 180^\circ$. In order to increase the visibility and to facilitate sample centering, a UV fluorescence lamp equipped with a fiber optic by Rapp optoelectronic (<http://www.rapp-opto.de>) was added to the crystallographic end-station (see Fig. 2*a*). A lens at the tip of the fiber optics produces a focused beam of broadband UV light centered around 280 nm that induces a strong fluorescence signal from proteins and DNA. Proteins emit a broad spectrum from 300 to 400 nm mainly originating from the aromatic side-chains. This fluor-

escence signal is then recorded with a standard high-resolution video microscopic optics and a CCD camera (large picture in Fig. 5). In this experiment the optics are not optimized to detect the fluorescence below 340 nm (cut-off for glass optics). Improving the optics will further increase the signal-to-noise ratio and hence the visibility. The protein crystal of approximate dimensions 0.3 mm \times 0.3 mm \times 0.2 mm and the loop are clearly visible with much higher contrast compared with the normal visible-light picture. Since the UV lamp can be switched on and off remotely, the combination of both pictures can be used to identify small and/or irregular crystals in the loop. A program for automatic crystal recognition called *VisionGrab* coded in C++ using the NI ImaqVision 6.0 library by National Instruments is under development. Whereas sophisticated image recognition can be a powerful tool for identifying crystals under visible light and has been successfully used to locate protein crystals in crystallization plates (Wilson, 2002; Spraggon *et al.*, 2002) as well as in loops (Andrey *et al.*, 2004), the color information may be more useful in the relatively diffuse UV fluorescence signal. Thus, *VisionGrab* uses the RGB color information (shown in blue in Fig. 5) followed by a thresholding and labeling function. A Canny edge-filtering (Canny, 1986) and size-filtering procedure is applied to determine separate objects (viewed in different colors on the right-hand side of Fig. 5). Then the centers of gravity are determined for all objects larger than the 20 μ m diameter of the rayon loop used here. In this favorable case, only the crystal remains and the center is marked with a cross. The computational time required is fractions of a second. It is clear that for more difficult cases, such as many small crystals in one big loop, more sophisticated methods may have to be used and the combination of different algorithms is currently in progress. The total time of semi-automatic centering is currently limited by the relatively slow φ movement to approximately 30 s assuming that four different φ angles are evaluated.

3.3. Two-dimensional barcode for sample tracking

Since the EMBL Hamburg Outstation serves a wide user community we developed a general and inexpensive barcode system that can be directly printed on the bottom of the magnetic caps (Fig. 6). The two-dimensional data matrix encodes alphanumerical numbers with a high redundancy in order to ensure readability under less-than-ideal conditions (*i.e.* ice formation). The barcode reader is located next to the storage dewar and, if utilized, the robot will stop for up to 2 s to read the code, adding approximately 3 s to the overall turnover time. A 14 \times 14 bit pattern, for example, encodes ten alphanumerical or 16 numerical values. In an attempt for further standardization the Structural Proteomics in Europe (SPINE)

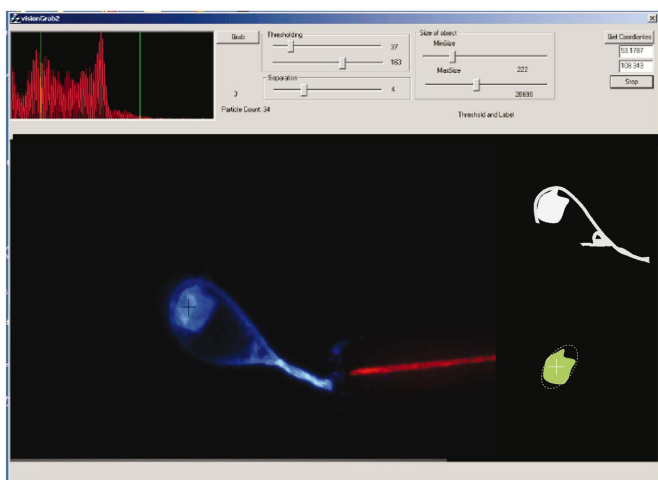


Figure 5
Protein test crystal mounted in a rayon loop (Teng, 1990) exposed to UV light. The picture in the center shows that the loop and crystal are clearly visible. The dark cross shows the center of the object as determined automatically with an initial version of *VisionGrab*. The small pictures on the right-hand side show different stages of object recognition.



Figure 6
Two-dimensional data matrix code for sample identification applied to the bottom of the Hampton-type magnetic caps.

consortium has decided to develop a common standard for the crystal holder based on the outer dimensions of the Hampton magnetic caps and sample tracking based on the barcode described here (details can be found at <http://www.spineurope.org>). Furthermore, MarResearch has further improved the reliability by establishing a laser-etching technique where the data matrix code is applied to the bottom and the alphanumeric values to the side of the cap. This method has the advantage that the code can also be read without a barcode reader. MarResearch has recently integrated a barcode reader into their desktop beamline (<http://www.marresearch.com>).

3.4. Initial tests with the entire system

The first prototype was installed and tested on beamline BW7B in the late summer of 2002. However, wide-ranging modifications of the storage dewar and the development of the overall control software did not allow an extensive test phase to be started before the late summer of 2003. At the beginning of 2004 the system entered its commissioning phase. During this time the software development and integration will continue. The first tests were performed using a variety of protein samples including tetragonal hen egg-white lysozyme crystals (crystal size up to 0.4 mm × 0.4 mm × 0.4 mm, unit-cell dimensions $a = b = 77.3 \text{ \AA}$, $c = 37.3 \text{ \AA}$), hexagonal non-phosphorylating glyceraldehyde dehydrogenase (crystal size 0.4 mm × 0.4 mm × 0.3 mm, unit-cell dimensions $a = b = 185.2 \text{ \AA}$, $c = 132.2 \text{ \AA}$) (Pohl *et al.*, 2002) and cubic oxoanion polyreductase (crystal size 0.1 mm × 0.1 mm × 0.1 mm, unit-cell dimensions $a = b = c = 191.3 \text{ \AA}$) (Polyakov *et al.*, 2003) protein crystals. In order to test the reliability of the system, pre-frozen crystals were repeatedly mounted, X-ray diffraction data were collected and subsequently the samples were dismounted. After every round the diffraction pattern was evaluated for any indications of crystal decay. The results of a typical experiment are summarized in Table 1. Here, five images in an oscillation range of 0.5° were recorded which, owing to the high symmetry, resulted in about 25% complete data sets. Then the crystal was dismounted, mounted and another five images were recorded. Even after several rounds, R_{sym} , $I/\sigma(I)$ and the mosaicity do not show any sign of crystal damage.

4. Conclusions

In summary, we have developed a fully automated crystallographic end-station including a robotic sample changer for the EMBL Hamburg protein crystallography beamline BW7B. The versatile and modular design described here allows for a straightforward adaptation to other beamlines at the EMBL Hamburg Outstation. The tunable beamline BW7A (Pohl *et al.*, 2001), for instance, has very recently been upgraded with the same automated end-station. The prototype described here has proven to reliably mount and dismount pre-frozen protein crystals. The open software architecture will enable us in the future to quickly integrate new developments towards a higher degree of automation. The obvious next steps are the integration of fully automated crystal recognition as well as auto-indexing of test images combined with an expert system that chooses the optimal parameters for data collection, such as the program *BEST* (Popov & Bourenkov, 2003). In addition, further upgrades on hardware components such as a new pre-mirror installed in March 2004 lead to a significant increase in brilliance and hence to shorter exposure times and thus faster data-collection times. We anticipate that, with the ongoing hardware and software developments, the automation project outlined in this report will significantly increase the efficiency of beamline BW7B.

Table 1

Effect of repeated mounting and dismounting on the crystal quality of oxoanion polyreductase (Polyakov *et al.*, 2003).

Five images in an oscillation range of 0.5° were collected to a resolution of 2.6 Å. Diffraction data were processed with *DENZO* and *Scalepack* (Otwinowski & Minor, 1997). The numbers in brackets refer to the last resolution shell.

No. of cycles	Completeness (%)	R_{sym} (%)	$I/\sigma(I)$	Mosaicity (°)†
1	25.6 (25.6)	5.7 (17.0)	9.8 (3.9)	0.18
2	26.4 (25.8)	5.6 (15.3)	11.5 (4.8)	0.19
6	25.3 (25.5)	5.3 (13.2)	11.4 (4.6)	0.19

† The values for mosaicity as refined with *Scalepack* represent a convolution with contributions from crystal mosaicity and instrumentation (beamline optics, source parameter) (Colapietro *et al.*, 1992). The maximum horizontal beam convergence is approximately 0.2°. Hence there is hardly any contribution from these crystals and only a significant increase in mosaicity caused by crystal decay would be noticeable.

We are very grateful to Esben Lorentzen and Alexander Popov for performing the test measurements using their precious protein crystals, and to Gert Rapp for his support during the UV fluorescence measurements. Furthermore, we would like to thank the entire PX staff of the EMBL Hamburg Outstation for their patience during the long test phase.

References

Abola, E., Kuhn, P., Earnest, T. & Stevens, R. C. (2000). *Nature Struct. Biol.* **7**, 973–977.

Andrey, P., Lavault, B., Cipriani, F. & Marin, Y. (2004). *J. Appl. Cryst.* **37**, 265–269.

Burley, S. K. & Bonanno, J. B. (2002). *Curr. Opin. Struct. Biol.* **12**, 383–391.

Canny, J. F. (1986). *IEEE Trans. Pattern Anal. Mach. Intell.* **8**, 679–698.

Cipriani, F. (2003). Personal communication.

Cohen, A. E., Ellis, P. J., Miller, M. D., Deacon, A. M. & Phizackerly, R. P. (2002). *J. Appl. Cryst.* **35**, 720–726.

Colapietro, M., Cappuccio, G., Marcante, C., Pifferi, A., Spagna, R. & Helliwell, J. R. (1992). *J. Appl. Cryst.* **25**, 192–194.

Earnest, T. E., Snell, G., Cork, C., Meigs, G., Nordmeyer, R., Cornell, E., Yegian, D. & Jin, J. (2002). *Acta Cryst.* **A58**, C56.

Heinemann, U., Illing, G. & Oschkinat, H. (2001). *Curr. Opin. Biotechnol.* **12**, 348–354.

Helliwell, J. R. (2002). *J. Synchrotron Rad.* **9**, 1–8.

Hendrickson, W. A. (2000). *Trends Biochem. Sci.* **25**, 637–643.

Hermes, C., Gehrmann, T., Jahn, D., Ristau, U., Robrahn, B. & Siambanis, T. (2004). *Proceedings of the Eighth International Conference on Synchrotron Instrumentation*. New York: AIP. (In the press.)

Ida, K., Yamamoto, M., Kumasaka, T., Ueno, G., Kanda, H., Yokozawa, Y., Sasaki, K. & Ishakawa, T. (2002). *Acta Cryst.* **A58**, C300.

Karain, W. I., Bourenkov, G. P., Blume, H. & Bartunik, H. D. (2002). *Acta Cryst.* **D58**, 1519–1522.

Kim, S. H. (1998). *Nature Struct. Biol.* **5**, 28–32.

McPhillips, T. M., McPhillips, M. C., Chiu, H. J., Cohen, A. E., Deacon, A. M., Ellis, P. J., Garman, E., Gonzales, A., Sauter, N. K., Phizackerley, R. P., Soltis, S. M. & Kuhn, P. (2002). *J. Synchrotron Rad.* **9**, 401–406.

Mitchell, E., Kuhn, P. & Garman, E. (1999). *Structure*, **7**, R111–R121.

Muchmore, S. W., Olson, J., Jones, R., Pan, J., Blum, M., Greer, J., Merrick, S. M., Magdalinos, P. & Nienaber, V. L. (2000). *Structure*, **8**, 243–246.

Ohana, J., Jacquamet, L., Joly, J., Bertoni, A., Taunier, P., Michel, L., Charrault, P., Pirocchi, M., Carpentier, P., Borel, F., Kahn, R. & Ferrer, J. L. (2004). *J. Appl. Cryst.* **37**, 72–77.

Otwinowski, Z. & Minor, W. (1997). *Methods Enzymol.* **276**, 307–326.

Pohl, E., Brunner, N., Wilmanns, M. & Hensel, R. (2002). *J. Biol. Chem.* **277**, 19938–19945.

- Pohl, E., Gonzales, A., Hermes, C. & van Silfhout, R. (2001). *J. Synchrotron Rad.* **8**, 1113–1120.
- Polyakov, K. M., Boiko, K. M., Tikhonova, T. V., Stekhanova, T. N., Antipov, A. N., Bourenkov, G. P., Popov, A. N., Lamzin, V. S. & Popov, V. O. (2003). *HASYLAB Annual Report 2003*. HASYLAB, Hamburg, Germany.
- Popov, A. N. & Bourenkov, G. P. (2003). *Acta Cryst.* **D59**, 1145–1153.
- Rosenbaum, G. (2000). Presentation at the *Workshop on Techniques for Automatic Mounting, Viewing and Centering of Pre-cooled Protein Crystals*, 11–12 May 2000, SSRL, Stanford, USA.
- Roth, M., Carpentier, P., Kaikati, O., Joly, J., Charrault, P., Pirocchi, M., Kahn, R., Fanchon, E., Jacquamet, L., Borel, F., Bertoni, A., Israel-Gouy, P. & Ferrer, J. L. (2002). *Acta Cryst.* **D58**, 805–814.
- Rupp, B., Segelke, B., Krupka, H. I., Lakin, T. P., Schäfer, J., Zemla, A., Toppani, D., Snell, G. & Earnest, T. (2002). *Acta Cryst.* **D58**, 1514–1518.
- Silfhout, R. van & Hermes, C. (1994). *Rev. Sc. Instrum.* **66**, 1818–1820.
- Spraggon, G., Lesley, S. A., Kreuzsch, A. & Priestle, J. P. (2002). *Acta Cryst.* **D58**, 1915–1923.
- Stevens, R. C., Yokohama, S. & Wilson, I. A. (2001). *Science*, **294**, 89–92.
- Sweet, R. M., Skinner, J. M. & Cowan, M. (2001). *Synchrotron Rad. News*, **14**, 5–11.
- Teng, T. Y. (1990). *J. Appl. Cryst.* **23**, 387–391.
- Terwilliger, T. C., Park, M. S., Waldo, G. S., Berendzen, J., Hung, L. W., Kim, C. Y., Smith, C. V., Sacchettini, J. C., Bellinzoni, M., Bossi, R., De Rossi, E., Mattevi, A., Milano, A., Riccardi, G., Rizzi, M., Roberts, M. M., Coker, A. R., Fossati, G., Mascagni, P., Coates, A. R., Wood, S. P., Goulding, C. W., Apostol, M. I., Anderson, D. H., Gill, H. S., Eisenberg, D. S., Taneja, B., Mande, S., Pohl, E., Lamzin, V., Tucker, P., Wilmanns, M., Colovos, C., Meyer-Klaucke, W., Munro, A. W., McLean, K. J., Marshall, K. R., Leys, D., Yang, J. K., Yoon, H. J., Lee, B. I., Lee, M. G., Kwak, J. E., Han, B. W., Lee, J. Y., Baek, S. H., Suh, S. W., Komen, M. M., Arcus, V. L., Baker, E. N., Lott, J. S., Jacobs, W. Jr, Alber, T. & Rupp, B. (2003). *Tuberculosis*, **83**, 223–249.
- Tucker, P. A. (2004). Personal communication.
- Wilson, J. (2002). *Acta Cryst.* **D58**, 1907–1914.
- Yamamoto, M. (2002). Presentation at the *International Conference on Structural Genomics*, Berlin, 8–9 October 2002, Satellite Workshop.
- Zhang, C. & Kim, S. H. (2003). *Curr. Opin. Chem. Biol.* **7**, 28–32.